

Pressure Effect on the Density of Water[†]

Chul Hee Cho,^{*,‡} Jacob Urquidi,[§] Surjit Singh,^{||} Seung C. Park,[‡] and G. Wilse Robinson^{⊥,‡}

Department of Chemistry, Natural Science Campus, Sungkyunkwan University, Suwon 440-746, Korea, Intense Pulsed Neutron Source, Argonne National Laboratories, 9700 South Cass Avenue, Argonne, Illinois, 60439-4814, HNC Software, Inc., 5935 Cornerstone Court West, San Diego, California 92121, and SubPicosecond and Quantum Radiation Laboratory, Department of Chemistry and Biochemistry, P.O. Box 41061, Texas Tech University, Lubbock, Texas 79409-1061

Received: September 26, 2001; In Final Form: April 23, 2002

A simple two-state structural model has been shown capable of quantitatively unifying oxygen-related properties of liquid water. The key variables, which remain invariant among all properties studied, are the pressure-/temperature-dependent densities and fractional compositions of the two contributing structures. In this paper, the pressure dependence of these variables for different temperatures is evaluated from density measurements of water for pressures up to 8 kbar. Data derived earlier from isothermal compressibilities provided only the leading term in the steep pressure dependence of these quantities. This leading term is found here to provide a good representation of the density of water in the pressure range from 1 to 1026 bar for $0 \leq t \leq 40$ °C. A correctly curved pressure dependence is introduced for the accurate description of pressure-dependent properties such as the refractive index of water and the pressure denaturation of proteins, where the experimental pressure range usually exceeds 1 kbar.

I. Introduction

Water, in its various physical states, shows many different aspects not closely related to its liquid-state properties. The qualitative and quantitative explanations of the various anomalous properties of liquid water have been presented using the two-state outer-neighbor structural bonding model. Temperature effects on the structure of liquid water,^{1,2} in addition to density,^{3,4} viscosity,⁵ refractive index⁶ anomalies, and isotope effects^{7,8} have been studied on the basis of this model. Apart from the effects of temperature, a beginning has also been made in understanding some of the pressure effects on water and their related anomalies.^{1,2,5,9,10}

The main purpose of this paper is to extend the previous two-state model to include the effects of pressure on liquid water. The advantage of doing this is that the domain of applicability of our approach is extended to another thermodynamic axis. This is necessary for extending our two-state physical picture of liquid water, which can then be applied to various issues involved in chemical and biological hydration.

II. Aspects of the Two-State Structural Model

Our approach to this water problem has always been to create a new, more realistic starting point. This has been done by building in, empirically at first, structural features that seem the most important. These structural features were derived from the known properties of the low and high-density amorphs,¹¹ then more explicitly from the crystalline forms of ice, in

particular ice-Ih and ice-II.^{12,13} This is an approach that has been promoted through the years by the crystallographic community¹⁴ for the understanding of local structures in liquids and glasses.

Despite the successes of our starting point for the study of liquid water, this explicit structural approach has been strongly criticized. For instance, it has been suggested that the terminology “ice-II-type” seems to ignore the wide array of other structures that could be involved. However, from the beginning,¹² all those structures have been considered in our papers, including the amorphous solid forms. The advantage of using ice-type bonding considerations for liquid water is that these structures are more precisely known than the structures of the amorphs. Furthermore, ice-II has the lowest energy structure of any of the moderately dense crystalline polymorphs¹⁴ and would be expected to be the most likely structure to grow in with increasing temperature, replacing the slightly more stable ice-Ih-type structure. In this regard, it is simply incorrect to obtain information about the relative stabilities of the possible ice-type packing configurations in the liquid from an examination of the phase diagram, or equivalently from the Gibbs free energies, of the crystalline forms. The reason for this has been discussed earlier,³ but will be repeated here for completeness.

Since crystalline ice-II has ordered hydrogens and the neighboring phases do not,¹⁵ the Pauling entropy^{16,17} of proton disorder $R \ln 3/2 = 3.3712 \text{ JK}^{-1} \text{ mol}^{-1}$ stabilizing ice-Ih is not present in crystalline ice-II. Since there is little chance of having ordered hydrogens in the ice-II-type structure in the liquid, the $P\Delta V$ term $\approx 830 \text{ Jmol}^{-1}$ in the ΔG free energy difference compensating for the lack of this entropy of disorder in crystalline ice-II would be expected to be much smaller, if not absent, in the liquid. In fact, at atmospheric pressure near 0 °C, the ΔG difference between the ice-Ih-type structure and the ice-II-type structure in the liquid is very likely well within the thermal energy of kT . Thus, it is not surprising that at this temperature and pressure there is approximately equal prob-

[†] Part of the special issue “G. Wilse Robinson Festschrift”.

^{*} To whom correspondence should be addressed. E-mail: chcho@chem.skku.ac.kr. Fax: +82-31-290-5375.

[‡] Department of Chemistry.

[§] Intense Pulsed Neutron Source.

^{||} HNC Software, Inc.

[⊥] SubPicosecond and Quantum Radiation Laboratory.

[#] Deceased September 7, 2000.

ability for the occurrence of these two bonding forms in the liquid, as verified from compositional determinations in our density analysis,³ and also very much in line with earlier¹⁴ and more recent¹⁸ proposals.

The structural importance of these two bonding forms in the liquid is that the O···O···O bond angle for the normal tetrahedral configuration is 109.5°, while, in the more dense polymorphs,¹⁴ some O···O···O angles are as small as 80°. ^{13–15} Since the energy difference between these structures is much smaller than the energy required to actually break a hydrogen bond, it can safely be assumed that this O···O···O angle bending only distorts but does not break hydrogen-bonds. The new feature in the liquid is thus the possibility of having highly bent intermolecular O···O···O bonds. Since the nearest neighbor hydrogen bonded O···O distances in all the ice forms are close to 2.75 Å, the small O···O···O angles in ice-II and the other moderately dense polymorphs bring the outer O-atom neighbors to within a much closer distance than the 4.5 Å non-hydrogen-bonded distance in ordinary tetrahedral ice-Ih.

The key feature here is the O···O next-nearest-neighbor distance of 3.2~3.5 Å, completely absent in ice-Ih but occurring in all the moderately dense forms of ice and the liquid.¹³ We believe that it is the presence in the liquid of the two very different outer-bonding structural characteristics that gives rise to the unusual properties of water. Models of water that do not explicitly promote these characteristics will find it difficult to reproduce accurately the actual properties of this substance over wide ranges of temperature, pressure, and interfacial perturbations.

III. Availability of Pressure–Volume Data for Water

Volume data for water at atmospheric pressure are known to about six significant figures for temperatures between 0 and 100 °C, and to five significant figures for supercooled temperatures down to –30 °C.^{3,19,20} However, for higher pressures, the data, mainly available only above 0 °C, scatter to not much better than four significant figure precision, and for pressures above 1 kbar, the errors seem worse.²¹ A persistent problem²² is the compression of the measuring apparatus itself and the failure to accurately compensate for this. Currently, therefore, it is not easy to choose pressure–volume data for water that remain reasonably good for high pressures.

According to an extensive investigation of over 8000 density measurements for elevated pressures, summarized in Table 6.2.2 of the Sato et al. paper,²¹ the data of Kell and Whalley²² consisting of 252 data points for temperatures greater than 0 °C and for pressures up to 1026 bar should have an overall average error in volume of no more than about 3×10^{-5} cm³g⁻¹. Data measured by Grindley and Lind²³ consisting of 560 data points for temperatures greater than 25 °C and for pressures up to 8 kbar were estimated²¹ to have an average error of about 1×10^{-4} cm³g⁻¹. See the phase diagram on page 93 of ref 15 for the temperature/pressure limitations of such measurements on the normal (not supercooled) liquid.

Although the freezing point of water is lowered under pressures of a few kbar,¹⁵ making the liquid more accessible for study, pressure–volume data for liquid water at elevated pressures and low temperatures are sparse, with about the only choice being the 61 data points reported by Aleksandrov, et al.²⁴ for temperatures between –9° and +5 °C and for pressures up to 1.01 kbar. Volume uncertainties in those data were said to be²¹ about 5×10^{-5} cm³g⁻¹. Other data reviewed in the Sato et al. paper²¹ were either not as accurate or did not cover the pressure/temperature range desired here.

Combining the raw experimental data of Kell and Whalley²² with those of Grindley and Lind²³ thus provides a set of fairly good experimental specific volumes for water in the temperature range upward of 0 °C and for pressures to 8 kbar. These data for temperatures to around 50 °C can be expressed within an uncertainty corresponding to a root-mean-square (rms) deviation Ω of better than 1×10^{-4} cm³g⁻¹ through use of a “single-state” Tait equation²⁵ relative to $P_0 = 1 \text{ atm} = 1.01325 \text{ bar}$

$$V_{\text{H}_2\text{O}}(T,P) = V_{\text{H}_2\text{O}}(T,P_0) \left[1 - \frac{P - P_0}{\kappa_0^{-1} + m(P - P_0) + n(P - P_0)^2} \right] \quad (1)$$

where $\kappa_0 = \kappa(T,P_0) = -V_0^{-1}(\partial V/\partial P)_{T,P_0}$ and $V_0 = V_{\text{H}_2\text{O}}(T,P_0)$ are the temperature-dependent isothermal compressibility and the specific volume of the liquid at $P = P_0$. The two parameters m and n take account of the compressibility change with increasing pressure.

The best fit of the combined experimental data from refs 22 and 23 is achieved for the single-state Tait equation when $m = 3.31938$ and $n = -4.541 \times 10^{-5}$, giving overall rms deviation $\Omega = 5.4 \times 10^{-5}$ cm³g⁻¹, with the largest errors in the range of $1 \sim 2 \times 10^{-4}$ cm³g⁻¹ for the data at the highest temperature and pressure limits considered in those experiments.

IV. Temperature and Pressure Dependence in the Two-State Model

The temperature/pressure-dependent specific volume of liquid water in terms of the two-state (I + II) outer bonding structural model is³

$$V(T,P) = f_{\text{I}}(T,P)V_{\text{I}}(T,P) + f_{\text{II}}(T,P)V_{\text{II}}(T,P) \quad (2)$$

where the fractional compositions $f_{\text{I}}(T,P)$ and $f_{\text{II}}(T,P)$ add to unity for a purely two-state representation. The temperature dependence of the compositions and volumes at atmospheric pressure has already been determined from a density analysis of both^{3,4} H₂O and D₂O in the temperature range from near –30° up to around +100 °C. For the highest temperatures covered in these analyses, it would be expected³ that the simple two-state model would have a reduced meaning because of the inevitable presence with increasing temperature of other contributions, including some sort of broken down hydrogen-bond structure. For this reason, and because the elevated pressure adds further uncertainty, we will consider a temperature range in this paper only up to the neighborhood of +50 °C.

The temperature and pressure dependence of the fractional compositions, f_{I} and f_{II} , as well as the two-state volumes, V_{I} and V_{II} , will now be discussed. As a first approximation, $f_{\text{I}}(T,P)$ can be assumed to be linear in pressure for a given temperature, so that

$$f_{\text{I}}(T,P) = f_{\text{I}}(T,P_0) + F_{\text{I}}^0(P - P_0) \quad (3)$$

with $f_{\text{II}}(T,P) = 1 - f_{\text{I}}(T,P)$ for the entire T,P range considered. The form for $f_{\text{I}}(T,P_0)$ used is³

$$f_{\text{I}}(T,P_0) = 1 - \tanh \left[\frac{A(T - T_0) + B(T - T_0)^2}{1 + C(T - T_0)} \right] \quad (4)$$

with parameters $A = 4.54866 \times 10^{-2} \text{ K}^{-1}$, $B = 3.6522 \times 10^{-4} \text{ K}^{-2}$, $C = 8.69196 \times 10^{-2} \text{ K}^{-1}$, and $T_0 = 225.334 \text{ K}$ for H₂O. The values of $f_{\text{I}}(T,P_0)$ derived from the earlier density analysis are given for selected temperatures in Table 1. In eq 3, $F_{\text{I}}^0 =$

TABLE 1: Quantities at $P_0 = 1.01325$ Bar Used To Determine the Leading Behavior of the Pressure Dependence for the Density of Liquid Water^a

$t, ^\circ\text{C}$	$f_I(T, P_0)$	$F_I^0(T, P_0)$	$\kappa_I(T, P_0)$	$\kappa_{II}(T, P_0)$	$V_I(T, P_0)$	$V_{II}(T, P_0)$
-30	.65174	-136.592	54.164	16.870	1.09625	.86698
-25	.61015	-113.974	54.878	17.706	1.09874	.87247
-20	.57574	-95.102	55.592	18.541	1.10123	.87795
-15	.54613	-79.354	56.306	19.377	1.10372	.88343
-10	.51993	-66.214	57.019	20.213	1.10621	.88891
-5	.49628	-55.250	57.733	21.049	1.10869	.89439
0	.47460	-46.102	58.447	21.884	1.11118	.89987
5	.45451	-38.468	59.161	22.720	1.11367	.90536
10	.43573	-32.098	59.874	23.556	1.11616	.91084
15	.41806	-26.783	60.588	24.392	1.11864	.91632
20	.40135	-22.348	61.302	25.227	1.12113	.92180
25	.38549	-18.648	62.016	26.063	1.12362	.92728
30	.37039	-15.560	62.729	26.899	1.12611	.93277
35	.35598	-12.983	63.443	27.735	1.12859	.93825
40	.34219	-10.834	64.157	28.570	1.13108	.94373
45	.32898	-9.040	64.871	29.406	1.13357	.94921
50	.31632	-7.543	65.584	30.242	1.13606	.95469
55	.30416	-6.294	66.298	31.078	1.13855	.96018
60	.29248	-5.252	67.012	31.913	1.14103	.96566
65	.28125	-4.382	67.726	32.749	1.14352	.97114
70	.27045	-3.656	68.440	33.585	1.14601	.97662

^a $F_I^0 = (\partial f_I / \partial P)_T$ for $P_0 = 1.01325$ bar (1 atm); the units of $F_I^0(T, P_0)$ and the compressibility factors $\kappa(T, P_0)$ are 10^{-6} bar⁻¹, while those of $V(T, P_0)$ are cm³g⁻¹.

$(\partial f_I / \partial P)_{T, P_0}$ is a negative quantity which, along with the individual isothermal compressibilities κ_I and κ_{II} , is already known at atmospheric pressure P_0 as a function of T from the earlier isothermal compressibility analysis,¹⁰ but recently corrected because of errors found in that analysis. See the listings in Table 1. As a function of temperature, F_I^0 exhibits close to an exponential form,¹⁰

$$F_I^0 = A' e^{-a(T-T_0)} \quad (5)$$

with $A' = -2.60350 \times 10^{-4}$ bar⁻¹ and $a = 0.036205$ K⁻¹.

As far as the two-state volumes V_I and V_{II} are concerned, the Tait equation²⁵ can again be used for each of these two components. Since V_0 and κ_0 for each of the two components are known from the earlier work,^{3,10} this procedure introduces just four new parameters to be assessed, m_I , m_{II} , n_I , and n_{II} . These four parameters, along with the known isothermal compressibilities κ_I and κ_{II} , when used in eq 1, give the desired V_I and V_{II} volumes as a function of temperature and pressure. The parameters used in evaluating f_I and f_{II} in previous work³ were provided to aide in the evaluation of the fractional contributions at different temperatures. The values of f_I (and consequently f_{II}) have attached to them a physical significance which is of fundamental importance to this two-state structural model and have remained unchanged in the analysis of every physical anomaly studied. It should be noted that D'Arrigo, et al. arrived at similar values via Raman spectroscopic methods.²⁶

V. Computational Details

Using eqs 1–3 with only the above four fitting parameters, the volume data of Kell and Whalley²² from $t = 0 \sim 40$ °C for pressures up to 1026 bar can be reproduced within a root-mean-square deviation $\Omega = 5.4 \times 10^{-5}$ cm³g⁻¹ for their data points. This is within the claimed²¹ experimental uncertainty. The resulting parameters for these experimental data are $m_I = 3.06470$, $m_{II} = 2.15700$, $n_I = 4.624 \times 10^{-4}$, and $n_{II} = -7.287 \times 10^{-4}$, with the switch in sign from n_I to n_{II} being the only worrisome feature.

Comparing the calculated values from these parameters with the experimental data of Aleksandrov et al.,²⁴ for temperatures -9° to $+5^\circ$ °C and pressures up to 1 kbar, indicates that those experimental volume data are very probably too small, by perhaps as much as 5×10^{-4} cm³g⁻¹ for the highest pressures that they studied.

Despite the above success at reproducing the Kell/Whalley²² T, P -dependent volumes for pressures up to 1 kbar, extension to higher pressures using the same parameters was found to give uniformly poor agreement with the data of Grindley and Lind,²³ where experimental pressures up to 8 kbar were studied. This is the reason that, as seen in eq 3, the values of f_I for lower temperature regimes decrease sharply with increasing pressures and at last become negative. Since one of the main purposes of the present work is to determine the compositional fractions f_I and $f_{II} = 1 - f_I$ and their respective volumes, V_I and V_{II} , up to moderately high pressures, eq 3 should be revised so as to have the correct curvature for f_I at high pressures.

In the analysis of the density data for pressures below 1 kbar, there seemed to be little need to consider the change of the pressure derivatives of f_I with increasing pressure. However, it would be expected that the magnitude of the negative $F_I = (\partial f_I / \partial P)_{T, P}$ would have to become smaller with increasing pressure as f_I itself becomes smaller. According to Table 1, the decreased magnitude of $F_I^0(T, P_0)$ with increasing temperature and decreasing $f_I(T, P_0)$ is seen to be very steep, so a similar behavior might be expected for increasing pressures. Therefore, it is merely assumed that the pressure effect on f_I has the same effect on the slope F_I as the temperature. In other words, as f_I decreases with increasing pressure, the magnitude of F_I decreases according to the instantaneous value of f_I . This introduces no new parameters, giving added weight to the simple assumption. Using this idea, the procedure used for calculating f_I from $f_I(T, P_0)$ is

$$f_I(T, P) = f_I(T, P_0) + \int_{P_0}^P F_I(T, P) dP \quad (6)$$

Since a high precision is needed, eq 6 was dealt with numerically using a finite difference method, with the value of $F_I(T, P)$ being continuously corrected as P increases and $f_I(T, P)$ decreases. The increment dP was tested at a number of different values, with 1, 0.1, and 0.01 bar all giving nearly identical results.

Using this finite difference method for the combined Kell/Whalley²² and Grindley/Lind²³ experimental data to 8 kbar, values of the required Tait parameters were found to be $m_I = 2.31603$, $m_{II} = 4.31121$, $n_I = -1.740 \times 10^{-5}$, and $n_{II} = -1.007 \times 10^{-4}$. These parameter values seem more reasonable than the ones obtained earlier considering only the low-pressure data of Kell and Whalley.²² In fact, their averages are not far from the parameter values found for the single-state Tait equation of eq 1 applied to all the data points considered in refs 22 and 23. The root-mean-square error Ω in this volume analysis was found to be 6.7×10^{-5} cm³g⁻¹, nearly equivalent to the single-state Tait equation results. Figure 1 shows the difference of the experimental specific volumes and the calculated values. One of the largest errors occurs at 1200 bar, at which pressure point is combined with two sets of experimental data from refs 22 and 23. It is also noted that the raw experimental data for the highest pressures at 0, 10, and 20 °C are not available because supercooling the liquid under such conditions may be difficult and not often attempted.

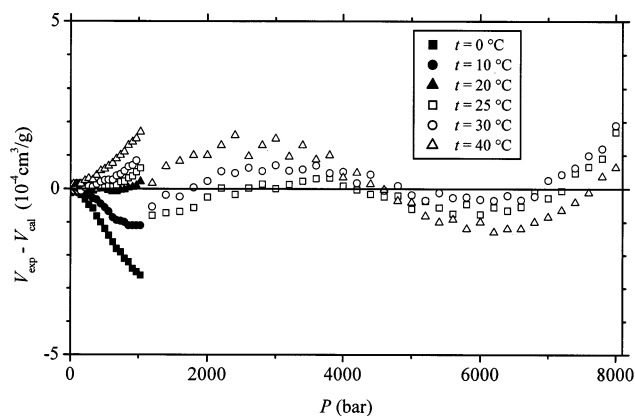


Figure 1. Comparison between the experimental specific volumes and the calculated values.

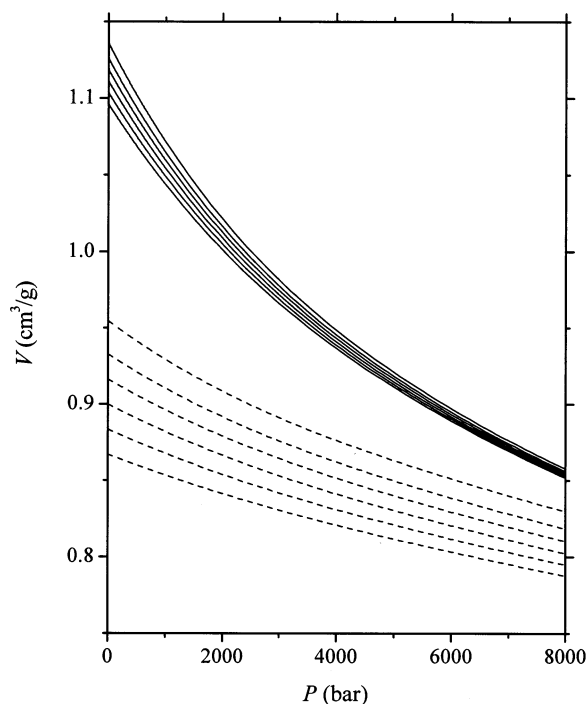


Figure 2. Two-state specific volumes V_I (solid lines) and V_{II} (dotted lines) as a function of temperature and pressure. The temperatures range from top to bottom for both V_I and V_{II} : 50, 30, 15, 0, -15, and -30 °C.

VI. Results and Discussion

The results for pressures up to 8 kbar are shown for selected temperatures in Figures 2 and 3 for the key variables $V_I(T,P)$, $V_{II}(T,P)$, and $f_I(T,P)$. Those quantities from this high pressure analysis are required so that increasingly prominent studies^{27,28} of biological pressure effects can be better assessed. The two-state specific volumes, $V_I(T,P)$ and $V_{II}(T,P)$, are plotted as a function of temperature and pressure in Figure 2. These volume data decrease with increasing pressure at a given temperature and do not cross each other.

Figure 3 presents the $f_I(T,P)$ results for pressure up to 8 kbar over the temperature range of -30 to +50 °C. There are two features to note about the f_I curves. First, on increasing pressure, the fraction f_I keeps on decreasing at a given temperature. This is reasonable as we expect the “open” structure to collapse with increasing pressure. Such phenomenon occurs on increasing temperature at a given pressure, as seen previously^{1,2,5,9,10} and is also apparent from the figure where the higher temperature curves are at the bottom.

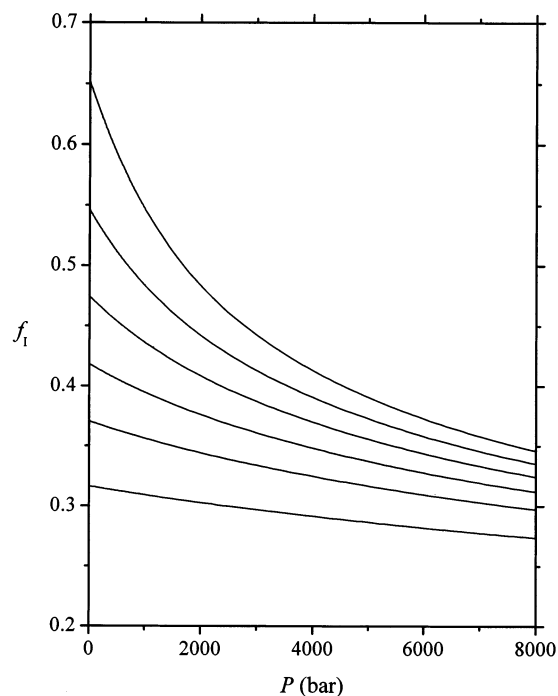


Figure 3. Fractions f_I of component I as a function of temperature and pressure. The temperatures range from top to bottom: -30, -15, 0, 15, 30, and 50 °C.

The second feature of note in Figure 3 is the apparent convergence of all the curves as pressure becomes high. This is also reasonable because at high enough pressures, there would be expected to be only the “closed” structure because the “open” structure would have collapsed into it.

One of the pressure effects resulting from the change of f_I (hence f_{II}) is the lowering of the temperature of maximum density (TMD) on increasing pressure. To see how our model compares to experiment, we plot various pressures against the TMD in Figure 4. The circles and the triangles are experimental data for H_2O ²⁹ and D_2O ,³⁰ respectively, and the dashed line is from ref 31. The solid line is from the two-state study presented here. The shapes of TMD from ref 31 and ours appear to be different from that shown for D_2O . It indicates that the two-state model as presented here may break down below around -15 °C. The deviation may be caused by a lack of experimental density data available below 0 °C at higher pressures. It is also worth noting that a comparison of the H_2O and D_2O properties under pressure would require a pressure isotope correction similar to the well documented correction required for temperature.^{32,33} Nevertheless, the pressure dependence of the basic quantities f_I , f_{II} , V_I and V_{II} of the two-state model as determined here can be applied to water in a biological environment.

VII. Concluding Remarks

The main purpose of this investigation has been to determine how the densities (ρ_I and ρ_{II}), the compositional fractions (f_I and f_{II}), and their pressure derivatives in the two-state model vary with pressure and temperature. We feel strongly that the functional forms of these variables play a central role in the understanding of pressure effects in surface chemistry and biology when water is the surrounding medium. We have already confirmed this expectation in recently published studies of pressure effects on the viscosity⁵ and the refractive index.⁶ In those studies, it was found that precisely the same functional forms with changing temperature and pressure of ρ_I , ρ_{II} , f_I , f_{II} ,

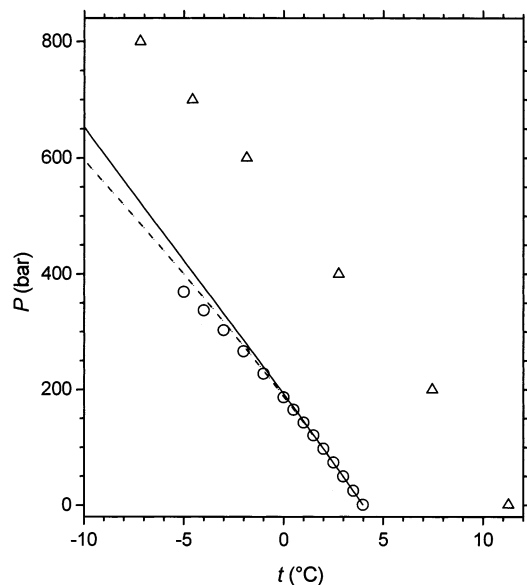


Figure 4. Temperature of maximum density of H₂O and D₂O as a function of pressure. For H₂O, the circles are experimental data from ref 29, the dashed line is from ref 31, while the solid line is the two-state result from the present study. Those two lines are extrapolated through $-10\text{ }^{\circ}\text{C}$. The triangles are experimental data for D₂O from ref 30.

$\partial f_l/\partial P$, and $\partial f_{II}/\partial P$ required for the pressure dependent density could be used to describe the seemingly diverse viscosity and refractive index properties of water as a function of temperature and pressure.

Many experiments of this type are suggested by the present work using pressure as a new variable. Because of the large numbers of water molecules involved, the thermodynamic differences between the I_h-type and II-type structures in the liquid, as their relative proportions change with temperature or pressure, could make a huge impact on the reactivity and equilibrium properties of such systems. For example, from a preliminary study,³⁴ it certainly appears that the hydration thermodynamics from these outerneighbor structural changes of the surrounding water with increasing temperature has modified the fragile thermodynamic balance between native and unfolded protein forms. This thermodynamic effect gives rise to both cold and heat denaturation of these systems.^{35–37} Because of similar thermodynamic shifts, the pressure denaturation of proteins³⁸ seems also to depend on these ideas. This work allows for their evaluation using the two-state structural model as it is applicable to the problem of protein hydration/denaturation.³⁹

Acknowledgment. C.H.C. acknowledges a BK21 Fellowship provided by the Ministry of Education of Korea. Acknowledged for financial support of this work are the R. A. Welch Foundation (D-0005 and D-1094), the Petroleum Research Fund (ACS-PRF 32253-AC6), and the Chemistry Support Fund at Texas Tech University. S.C.P. also thanks the KOSEF for partial financial support (KOSEF-1999-1-121-001-5).

References and Notes

- Urquidi, J.; Singh, S.; Cho, C. H.; Robinson, G. W. *Phys. Rev. Lett.* **1999**, *83*, 2348.
- Robinson, G. W.; Cho, C. H.; Urquidi, J. *J. Chem. Phys.* **1999**, *111*, 698.
- Vedamuthu, M.; Singh, S.; Robinson, G. W. *J. Phys. Chem.* **1994**, *98*, 2222.
- Vedamuthu, M.; Singh, S.; Robinson, G. W. *J. Phys. Chem.* **1994**, *98*, 8591.
- Cho, C. H.; Urquidi, J.; Robinson, G. W. *J. Chem. Phys.* **1999**, *111*, 10171.
- Robinson, G. W.; Cho, C. H.; Gellene, G. I. *J. Phys. Chem. B* **2000**, *104*, 7179.
- Vedamuthu, M.; Singh, S.; Robinson, G. W. *J. Phys. Chem.* **1996**, *100*, 3825.
- Cho, C. H.; Urquidi, J.; Singh, S.; Robinson, G. W. *J. Phys. Chem. B* **1999**, *103*, 1991.
- Urquidi, J.; Cho, C. H.; Singh, S.; Robinson, G. W. *J. Mol. Struct.* **1999**, *485–486*, 363.
- Vedamuthu, M.; Singh, S.; Robinson, G. W. *J. Phys. Chem.* **1995**, *99*, 9263. See Table 1 of the present paper for corrected values of the compressibility parameters.
- Mishima, O.; Calvert, L. D.; Whalley, E. *Nature* **1984**, *310*, 393.
- Bassez, M.-P.; Lee, J.; Robinson, G. W. *J. Phys. Chem.* **1987**, *91*, 5818.
- Cho, C. H.; Singh, S.; Robinson, G. W. *J. Chem. Phys.* **1997**, *107*, 7979.
- Kamb, B. In *Structural Chemistry and Molecular Biology*; Rich, A., Davidson, N., Eds.; W. H. Freeman: San Francisco, 1968; pp 507–542.
- Eisenberg, D.; Kauzmann, W. *The Structure and Properties of Water*; Oxford University Press: London, 1969.
- Pauling, L. *J. Am. Chem. Soc.* **1935**, *57*, 2680.
- Nagle, J. F. *J. Math. Phys.* **1966**, *7*, 1484.
- Soper, A. K.; Ricci, M. A. *Phys. Rev. Lett.* **2000**, *84*, 2881.
- Kell, G. S. *J. Chem. Eng. Data* **1975**, *20*, 97.
- Hare, D. E.; Sorensen, C. M. *J. Chem. Phys.* **1987**, *87*, 4840.
- Sato, H.; Watanabe, K.; Levelt Sengers, J. M. H.; Gallagher, J. S.; Hill, P. G.; Straub, J.; Wagner, W. *J. Phys. Chem. Ref. Data* **1991**, *20*, 1023.
- Kell, G. S.; Whalley, E. *J. Chem. Phys.* **1975**, *62*, 3496.
- Grindley, T.; Lind, J. E., Jr. *J. Chem. Phys.* **1971**, *54*, 3983.
- Aleksandrov, A. A.; Khasanshin, T. S.; Larkin, D. K. *Russ. J. Phys. Chem.* **1976**, *50*, 231.
- Hayward, A. T. *J. Brit. J. Appl. Phys.* **1967**, *18*, 965.
- D'Arrigo, G.; Maisano, G.; Malmace, F.; Migliardo, P.; Wanderlingh, F. *J. Chem. Phys.* **1981**, *75*, 4264.
- Heremans, K.; Smeller, L. *Biochim. Biophys. Acta* **1998**, *1386*, 353.
- Mentré, P.; Hamraoui, L.; Hui Bon Hoa, G.; Debey, P. *Cell. Mol. Biol.* **1999**, *45*, 353.
- Aleksandrov, A. A.; Okhotin, V. S.; Ershova, Z. A. *Therm. Eng.* **1981**, *28*, 249.
- Kanno, H.; Angell, C. A. *J. Chem. Phys.* **1980**, *73*, 1940.
- Pruss, A. B.; Wagner, W. In *Proceedings of the 12th International Conference on the Properties of Water and Steam*; White, H. W., Jr., Sengers, J. V., Neumann, D. B., Bellows, J. C., Eds.; Begell House Publishers: New York, 1995; pp 66–77.
- Tomberli, B.; Benmore, C. J.; Egelstaff, P. A.; Neuefeind, J.; Honkimäki, V. *J. Phys.: Condens. Matter* **2000**, *12*, 2597.
- Root, J. H.; Egelstaff, P. A.; Hime, A. *Chem. Phys.* **1986**, *109*, 437.
- Robinson, G. W.; Cho, C. H. *Biophys. J.* **1999**, *77*, 3311.
- Makhatadze, G. I.; Privalov, P. L. *Adv. Protein Chem.* **1995**, *47*, 307.
- Privalov, P. L. *Crit. Rev. Biochem. Mol. Biol.* **1990**, *25*, 281.
- Ibarra-Molero, B.; Makhatadze, G. I.; Sanchez-Ruiz, J. M. *Biochim. Biophys. Acta* **1999**, *1429*, 384.
- Zipp, A.; Kauzmann, W. *Biochemistry* **1973**, *12*, 4217.
- Robinson, G. W.; Urquidi, J.; Singh, S.; Cho, C. H. *Cell. Mol. Biol.* **2001**, *47*, 757.